2016 American Control Conference (ACC)
Boston Marriott Copley Place
July 6-8, 2016. Boston, MA, USA

Noise Induced Transport at Microscale Enabled by Optical Fields

Shreyas Bhaban*,[1], Saurav Talukdar*,[2] and Murti Salapaka[1]
*Both authors have contributed equally

***Abstract*— Transport at the micro scale is an essential aspect for many emerging areas including manufacturing systems at the nanoscale. Transfer of beads decorated with cargo under the influence of optical fields provide an attractive means of such transport. Physical models that describe beads in optical fields under the influence of thermal noise are available which yield a qualitative understanding of the bead motion; however, it is difficult to arrive at models that provide quantitative agreement. The first contribution of the article is the determination of a model of a bead under a static field realized by optical forces where the model can be used to predict the motion of the bead under a time-varying optical potential with high fidelity. Close agreement between model based Monte Carlo simulations and experimental observations is seen. The other contribution is a strategy for directed transport of micron-sized particles that utilizes the proposed models to arrive at conclusions which are experimentally verified and easy to implement. The effectiveness of this transport mechanism is justified based on splitting probability computations. Applications to transport of cargo across multiple locations and transport of multiple cargo are experimentally demonstrated.**

Keywords : Optical trap, Langevian equation, harmonic potential, double well potential, thermal noise induced transport, nano scale transport

I. INTRODUCTION

New abilities of measuring and manipulating matter at the nanoscale hold the promise of designing and fabricating materials with unparalleled specificity, by employing rational control of matter at the nano and micro scale. An important need for such a promise to materialize is that of transporting micron sized or smaller particles from sources to destinations in an efficient manner.

Unlike in macro scale processes, thermal noise [1] plays a significant role in guiding and determining the results of processes (such as transport) and shapes the matter at the nanometer and smaller scales. With advances in nanotechnology and nanoscience, the effects of thermal noise can be measured and thus nano/micro scale systems provide a means to unravel the fundamental mechanism at play at smaller scales ([2], [3]). In this article a key focus is on the transport of particles using optical forces and noise. It is envisaged that spherical particles are decorated with the cargo/material to be transported and potential landscapes are created using optical fields to provide motion in the desired direction. Here it is impractical to pick and move each cargo from source to destination as typically the number of cargo is very large. The transport of multiple particles can be achieved in an open-loop manner or can be guided by feedback ([4], [5]), [6]. In many strategies such as Brownian Ratchets [5] the effects of noise are used for enabling transport; thus it is imperative to quantitatively analyze the effects of noise on transport modalities. A key step is to obtain models that are realistic which can be employed with quantitative precision to design protocols for efficient transfer of particles at the micron scale.

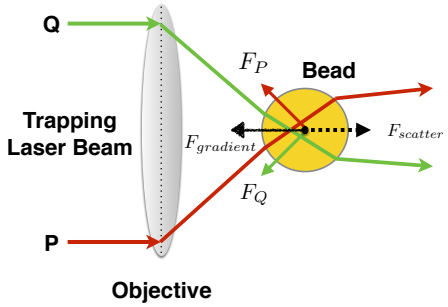

Fig. 1. Representation of bead in a single optical trap. The equivalent gradient force $F_{gradient}$ balances the destabilizing scattering force $F_{scatter}$, creating a stable equilibruim point near the focus of the objective.

Arthur Ashkin [7] demonstrated that when a laser beam is passed through an objective with appropriately high numerical aperture , the momentum transfer from the reflected and refracted rays onto microscopic particles in the vicinity of the focus generates two kinds of forces on the particle. As is seen in Fig. 1, the gradient forces, that result from the Gaussian intensity profile of the laser, balance the destabilizing scattering force of the laser that push the particle away from the focus, creating an equilibrium point. Furthermore, if the particle is dislodged from that point, it experiences a restoring force that pulls it back towards the focal point, indicating that it is a stable equilibrium point. A particle in such a stable trap experiences restoring forces that vary linearly with small displacements away from the focus, indicating potential of parabolic nature in the region. Optical trapping is used to study transport of cells, separation of microscopic objects and many other processes [8]. However, the force felt by the particle in an optical trap has a complex relationship with the shape of the particle, the relative refractive index of the particle with respect to its surroundings and on the relative position of the focal spot of the laser beam with respect to the particle center of mass. For understanding transport of particles, the force field generated by the optical potentials has to be quantitatively understood over large excursions of the bead positions and thus linear approximations do not suffice. Moreover, the transport is significantly affected by thermal noise in the optical potential where a good understanding of the potential is crucial for

[1]Shreyas Bhaban and Murti Salapaka are with Department of Electrical and Computer Engineering, University of Minnesota Twin Cities, Minneaplis, MN 55455, USA bhaba001@umn,edu, murtis@umn.edu
[2]Saurav Talukdar is with the Department of Mechanical Engineering, University of Minnesota Twin Cities, Minneaplis, MN 55455, USA taluk005@umn.edu

making assessments on the effects of thermal noise. Although the qualitative understanding and underlying principles for such particle behavior are well understood, it is difficult to arrive at a realistic model of this system using first principles.

Noise induced transport strategy based on realizing periodic asymmetric potentials is also hypothesized to be the underlying transport mechanisms for motor proteins like kinesin [9]. Arrays of micron-scale potential wells, generated with holographic optical tweezers [10] is shown to enable transport. Potential profiles with multiple minimas, such as a parabolic double well potential, represent an important category of conservative force field which is used to analyze structural phase transitions [11], isomerization reactions [12], behavior of quantum mechanical systems [13], 1 bit memory [14] and many other important physical systems. Studies and theories on fundamental sources of noise that include detailed studies of Brownian ratchet mechanisms [5], limits on the work required to erase bits [15] and recent studies on non-equilibrium statistical mechanics [16] can be evaluated (where deeper insights can be sought) using optically realized potentials with multiple minima.

In earlier efforts [17] the trap was modeled using a cubic nonlinearity where linear and nonlinear feedback strategies were employed to reduce the variance of the bead in the trap. In our article, the potential felt by a bead under single optical trap is characterized from experimental data and is used it to arrive at models for a potential field that results when the trap position is controlled and shared between different locations by time multiplexing of the laser. It is utilized to create an effective double well potential, following which a micro scale transport strategy is presented where thermal noise is used to achieve directed transport. It is achieved by creating an asymmteric double well potential by multiplexing for a longer duration in one location as compared to other and justified based on computations of splitting probabilities [18]. Furthermore, the proposed method is easier to implement experimentally as it involves simple multiplexing. A significant emphasis of the article is to determine models which yield *quantitative agreement* with experiment. Models to realize more complex transport strategies where quantitative estimates, for example, of rates of transitions can be determined are provided. Moreover, the detailed description of effects of thermal noise presented here can be used to obtain insights into other naturally occurring nanoscale systems, such as motor-proteins, where it is hypothesized that noise induces transport.

In Section II we present a brief description of our optical tweezer setup. Section III describes the characterization of a bead in a single well potential. In Section IV we use the insights from Section III to develop models for a bead in a double well potential and present experimental validation. Section V deals with transport of a bead by creating asymmetric double well potential with experimental verification followed by Conclusions in Section VI.

II. Bead in a Single Well

A. Experimental Setup

Experimental data presented in this article is obtained using a custom built optical tweezer setup as described in [19], [20].

B. Modeling

In this section a realistic model of a bead in a viscous medium in an optical trap is presented. The key objective is to obtain a model which is capable of providing a quantitative match with experimental observations. A dielectric bead in a viscous fluid undergoes free Brownian motion [18], where, the bead represents the system of interest and the viscous fluid around the bead acts like a heat bath [21]. Under the influence of a conservative force field the dynamics of the bead in a viscous fluid is modeled by the Langevin equation [1].

The stiffness of the trap depends on the location of the center of mass with respect to the trap location. A Hookean spring approximation holds for excursions of the bead away from the trap location till a threshold is reached beyond which the trapping force on the bead decays rapidly to zero. A model for the potential experienced by a bead in an optical trap $U(x)$ which comprises of a reference energy U_r, harmonic potential region until a width w and a flat potential surface beyond this width is described by,

$$U(x) = \begin{cases} \frac{1}{2}kx^2 + U_r & \text{if } |x| \leq w \\ \frac{1}{2}kw^2 + U_r & \text{if } |x| > w. \end{cases} \quad (1)$$

Here, k denotes the trap stiffness which can be altered by changing parameters like intensity of the laser. Although there exists a non-harmonic region beyond the width w [17], the bead spends insignificant amount of time in the non-harmonic region, hence the flat approximation is reasonable.

The discretization of Brownian motion dynamics and Langevin dynamics using stochastic calculus [18] along with the overdamped dynamics approximation leads to (2) and (3) respectively [22],

$$x(t+\delta t) = x(t) + \sqrt{\frac{2k_BT}{\gamma}dt}\ \nu(t), \quad (2)$$

$$x(t+\delta t) = x(t) - \frac{k}{\gamma}x(t)\delta t + \sqrt{\frac{2k_BT}{\gamma}\delta t}\ \nu(t), \quad (3)$$

where, γ is the viscous friction coefficient, k_B is the Boltzmann constant, T is the temperature of the heat bath and $\nu(t) \in \mathcal{N}(0,1)$. Here, $\mathcal{N}(0,1)$ denotes the standard normal distribution. As long as the bead is under the influence of the potential, its dynamics is modeled by (3). Outside the influence of the potential (i.e outside the width w) the bead undergoes free Brownian motion and its dynamics is modeled by (2).

A model for the potential beyond the harmonic range is needed for addressing transport issues because the bead needs to go through large excursion from the potential minima where the linear approximation does not hold. The simple model of a parabolic potential followed by a no force regime is evaluated below using simulations and experiments. Equations (2) and (3) are used to simulate the dynamics of a bead in an optical trap using Monte Carlo methods and are validated with experiments.

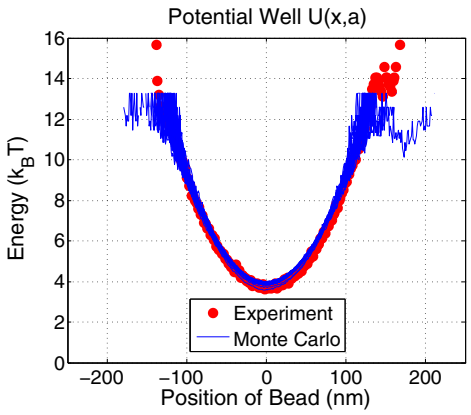

Fig. 2. Potential for single well obtained from Monte Carlo simulatios and experiments. Experimental observations and Monte Carlo simulation predictions match well.

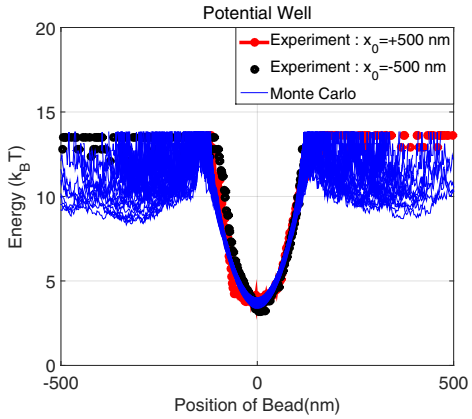

Fig. 3. Estimating nature of single potential well beyond a distance $w \approx 150\ nm$ from the minima

C. Experiments

Experimental data is obtained using a custom built optical tweezer that is used to trap a spherical polystyrene bead ($1\ \mu m$ diameter). The bead position data is measured using a quadrant photodiode (QPD). The spatial probability density of the bead in equilibrium is given by,

$$P(x) = C\ \exp\ (-\frac{U(x)}{k_B T}),$$

where C is a normalization constant. It follows that,

$$U(x) = -\ \ln\ (\frac{P(x)}{C}). \tag{4}$$

Here, the time scales of the experiment are long enough to allow the bead to attain thermal equilibrium. The above equation computes potential energy in units of $k_B T$. The probability distribution and potential for a bead in a single potential well (Fig. 2) is obtained after tracking the bead position (in a single optical trap) for a sufficiently long time (thus allowing it to equilibrate). It shows a parabolic nature until a finite distance $w \approx 150\ nm$ from the minima. To estimate the nature of the potential beyond w, the bead is released from an initial location of $\pm 500\ nm$ and its position is tracked from the moment of release till the bead attains equilibrium. The bead effectively sees a flat potential beyond w (see Fig. 3), indicating that beyond a distance w from the minima of $U(x)$, the bead dynamics are *primarily* dictated by thermal noise with no influence from the optical trap. The bead is seen to spend little time in the non-harmonic region of the potential, justifying the approximation by a constant beyond the harmonic range. The trap stiffness $k = 0.0044\ pN/nm$ is obtained from the bead position data using the Equipartition Theorem [23],

$$\frac{1}{2}k\langle x^2\rangle = \frac{1}{2}k_B T, \tag{5}$$

where the room temperature T is 300 K , viscosity $\eta = 8.9 \times 10^{-4} Pa.s$ [24] which results in $\gamma = 8.3 \times 10^{-9} Ns/m$.

D. Simulation Results

The integration time step $\delta t = 10^{-5} s$ is such where $\delta t \ll \frac{\gamma}{k} \sim 10^{-3} s$. Note that $\frac{\gamma}{k}$ represents the time constant in (3). The system parameters k, γ and w for simulations are obtained from experiments. The simulation results of reconstructed potentials $U(x)$ as shown in Fig. 2 are obtained by simulating the trajectories of 100 particles. The position trajectory of each particle is used to obtain the overall effective potential experienced by the bead using equation (4). It is seen in Fig. 2 that the potential reconstructed from the Monte Carlo simulations is in very close agreement with the one obtained from experiments.

In Fig. 3 potential reconstructed from the trajectories of 100 particles collectively with half of them initialized at $x(0) = 500\ nm$ and other half from $x(0) = -500\ nm$ is presented. It is evident that beyond the harmonic regime, both experiments and simulation exhibit a predominantly flat potential. Note that the transition region for both experiments and Monte Carlo simulations is difficult to reconstruct from position data, as the bead spends very less time in the transition region [25].

Thus, it can be concluded that the model proposed above matches experimental observations and lays the foundation for studying the dynamics of a bead in multiple wells as described below.

III. Bead in a Double Well Potential

A double well potential can be realized by focusing the laser alternately at two different positions, $d, -d$ with a high switching rate. The time scales of switching need to be less than that of the characteristic time of the bead dynamics. In our setup switching takes place in the order of $10\ \mu s$ while the time constant of the bead dynamics is of the order of $1\ ms$. The ON time of the laser at d and $-d$ needs to be same in order to realize a symmetric double well potential. Modulating the ON times at these locations results in the creation of asymmetric potential wells, with a deeper well being formed at the location with higher ON time. Understanding of the dynamics of a bead in a double well potential is fundamental to the development of the noise induced transport strategy presented in the following section.

The model developed for a bead in single well potential in the previous section is used to study the dynamics of a bead in a symmetric double well potential realized by multiplexing equally at locations d and $-d$. Let $l(t)$ and

$r(t)$ be binary variables where $l(t) = 1$ if the laser at $-d$ is ON i.e. $t \in [0, T_{ON}]$, else $l(t) = 0$. Similarly $r(t) = 1$ if the laser at $+d$ is ON i.e. $t \in [T_{OFF}, T_{total}]$, else $r(t) = 0$. One switching cycle lasts for $T_{total} = T_{ON} + T_{OFF}$. The potential $V(x, r(t), l(t))$ is given by :
$V(x, r(t), l(t))$

$$= \begin{cases} \frac{1}{2}k(x-d)^2 + U_r, & \text{if } |x-d| \leq w \text{ and } r(t) = 1 \\ \frac{1}{2}k(x+d)^2 + U_r, & \text{if } |x+d| \leq w \text{ and } l(t) = 1 \\ \frac{1}{2}kw^2 + U_r, & \text{otherwise.} \end{cases} \tag{6}$$

where, k is the trap stiffness (determined experimentally using equipartition theorem), U_r is a constant reference potential energy. The time constant of the laser switching is significantly faster ($\sim \mu s$) than the time constant of the bead dynamics ($\sim ms$). The potential $V(x, r(t), l(t))$ as described in (6) is the instantaneous potential experienced by the bead. This is in the time scales of order of switching of the laser focus. The discretized Langevin and free Brownian dynamics of the overdamned bead under the influence of $V(x, r(t), l(t))$ are summarized in (7), (8) and (9).

$$x(t+\delta t) = x(t) - \frac{k}{\gamma}(x(t) - d)\delta t + \sqrt{\frac{2k_BT}{\gamma}\delta t}\ \nu(t), \tag{7}$$
if $r(t) = 1$ and $|x - d| \leq w$

$$x(t+\delta t) = x(t) - \frac{k}{\gamma}(x(t) + d)\delta t + \sqrt{\frac{2k_BT}{\gamma}\delta t}\ \nu(t), \tag{8}$$
if $l(t) = 1$ and $|x + d| \leq w$

$$x(t+\delta t) = x(t) + \sqrt{\frac{2k_BT}{\gamma}\delta t}\ \nu(t), \text{ otherwise.} \tag{9}$$

Fig. 4 shows the effective potential determined from Monte Carlo simulations by analyzing realizations of paths taken by 200 particles initialized randomly between the right and left potential wells and using (4).

To create the potential experimentally, the laser used to create single optical trap is now multiplexed between two points d and $-d$. At a given position $-d$ distance away from the center, the laser is kept on for a time T_{ON} and off for T_{OFF} with the laser at d ON when the laser is OFF at $-d$. In the experiment we set the duty ratio $T_{ON}/T_{total} = 0.5$ with $T_{ON} = 120\ \mu s$ which is less than the time constants of the bead (order of ms). Equal ON and OFF times creates identical potential wells at both locations.

Fig. 4 shows the experimental realization of a double well potential for $d = 700\ nm$ with the minimas formed at a distance $688\ nm$ from the origin. Data for the right well is obtained after the bead is first initialized at $700\ nm$ and then the laser is rapidly switched between d and $-d$. For the left well, the initialization is done at $-700\ nm$. Similar to use of (4) for determining potential from simulation data, (4) is used to determine double well potentials from experimental data. Thus, first the model for single potential well is determined from experimental data and used to predict the potential that

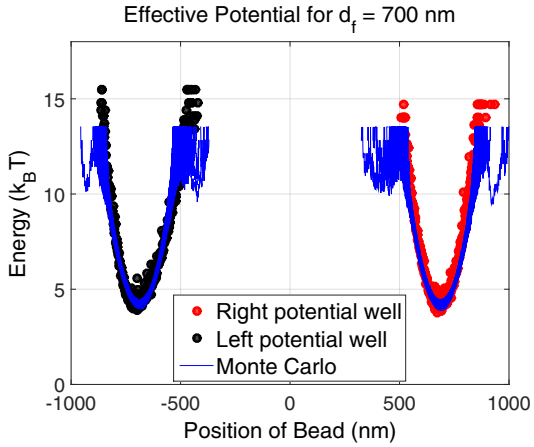

Fig. 4. Double well potential for $d = 700\ nm$ obtained using Monte Carlo simulations and experiments. Close match between Monte Carlo simulations and experiments is seen.

results when the laser is switched between d and $-d$. A close match between the effective potentials reconstructed using experimental data and Monte Carlo simulations is seen in Fig. 4. Note that though the linear range of PSD is limited to $\pm 250\ nm$, bead position data beyond this limit till $\pm 1000 nm$ is obtained using a multi-layered neural network [26].

It is observed in Fig. 4 that the barrier height for both the potential wells is quite high for it to be quickly overcome by noise. Thus when the separation between the wells is significant and the wells are sufficiently stiff, noise induced transition of the bead from one well to the other will take very long (as compared to the time scales of the experiment), explaining why we did not observe any such events. Note that the widths of the two wells is $\approx 150\ nm$ on either sides of the minima, which is comparable with the single well potential observed in Fig. 2.

In order to determine how the inter trap distance given by $2d$ affects the nature of the average potential created, a Monte Carlo simulation with $d = 50nm$ for 100 particles is performed (entirely determined by the single well characterization developed in the previous section) and the results are shown in Fig. 5. The bead effectively experiences a single well potential. To test this experimentally the laser is now multiplexed between locations $50\ nm$ and $-50\ nm$. Fig. 5 indicates that effectively a single potential well is created, showing a good match with Monte Carlo results. Thus it can be inferred that the laser needs to be switched between locations sufficiently far away for two parabolic potentials to be realized as is satisfied in the case of Fig. 4.

When the separation between the traps is significant, the average potential experienced by the bead due to fast switching of the laser (at constant laser power) $\tilde{V}(x)$ can be shown to satisfy the relation in (10), where x is the position of the bead with reference to the origin as shown in Fig. 4. $\tilde{V}(x)$ is the potential experienced by the bead in time scales of the order of time constant of the bead ($\sim 1ms$).

$$\tilde{V}(x) = \begin{cases} \frac{1}{2}\tilde{k}(x-d)^2 + U_r, & \text{if } |x-d| \leq w \\ \frac{1}{2}\tilde{k}(x+d)^2 + U_r, & \text{if } |x+d| \leq w \\ \frac{1}{2}\tilde{k}w^2 + U_r, & \text{otherwise} \end{cases} \tag{10}$$

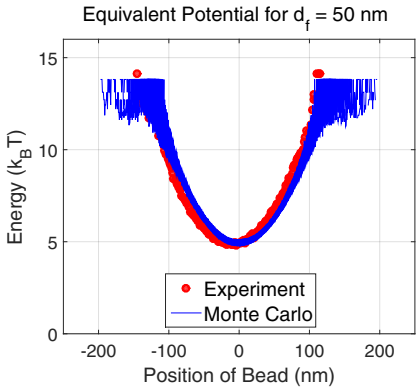

Fig. 5. Equivalent potential for $d = 50\ nm$ obtained using Monte Carlo simulations and experiments. A close match between experiments and Monte Carlo simulations is seen.

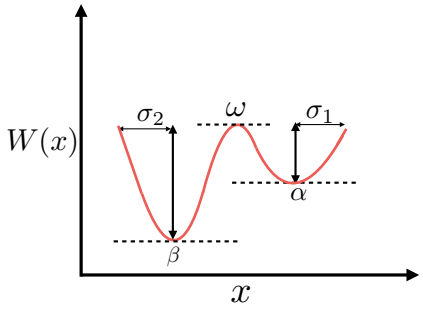

Fig. 6. A bistable potential with two parabolic wells with stable equilibrium points of α and β and of width σ_1 and σ_2 respectively. The point ω represents the barrier point.

Note that the stiffness $\tilde{k}$ in (10) is different from k in (6) beacause $\tilde{k}$ is the average stiffness of the trap over the switching cycles which includes phases where the laser was ON and OFF at $\pm d$. During the OFF phase the trap stiffness is zero and hence it is expected that $\tilde{k} < k$. Experimentally $\tilde{k} = 0.0034\ pN/nm$ whereas $k = 0.0044\ pN/nm$.

A clear conclusion that can be reached is that the single well characterization developed in the previous section can be used to predict quantitatively the optical forces felt by the bead under different strategies of time-multiplexing the laser and creating different profiles. The quantitative agreement holds for large excursions of the bead and is not restricted to deviations about the local minima of the potentials. Such models become useful for understanding noise induced transport.

IV. NOISE INDUCED TRANSPORT

In this section, backed by an analytical explanation, a method for transport enabled by using noise is reported. The probability density $P(x,t)$ of a bead in a viscous meduim under a influence of a potential $\tilde{V}(x)$ is described by the following Fokker-Planck equation [27]:

$$\partial_t P(x,t) = \frac{1}{\gamma}\partial_x[\tilde{V}'(x)P(x,t)] + D\partial_x^2 P(x,t), \qquad (11)$$

where, $D = \frac{k_B T}{\gamma}$. The stationary probability density is $P_s(x) = C\exp[\frac{-\tilde{V}(x)}{k_B T}]$ where C is a normalization constant.

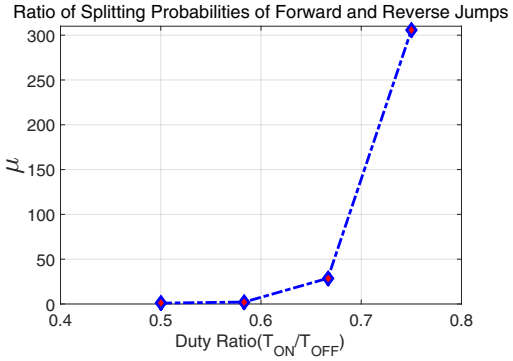

Fig. 7. Ratio of splitting probabilities μ against duty ratio obtained using Monte Carlo simulations. As the duty ratio increases μ increases exponentially.

In Fig. 6 a potential $W(x)$ is illustrated with α and β being stable equilibrium points. Both wells are parabolic and it is desired to transport the bead from α to β. The probabilities of transitioning to β (forward transition) and α (reverse transition) from an intermediate point x_0 are called *splitting probabilities* and are denoted by $\pi_\alpha(x_0)$ and $\pi_\beta(x_0)$ respectively. The splitting probabilities are used to arrive at a condition for transport from α to β.

Theorem 4.1: The splitting probabilities are given by

$$\pi_\alpha(x_0) = \frac{\int_{x_0}^{\beta} p_s(x)^{-1}dx}{\int_{\alpha}^{\beta} p_s(x)^{-1}dx}, \pi_\beta(x_0) = \frac{\int_{a}^{x_0} p_s(x)^{-1}dx}{\int_{\alpha}^{\beta} p_s(x)^{-1}dx}.$$

Proof: See [18] for the proof. ■

Note that $\pi_\alpha(x_0)+\pi_\beta(x_0) = 1$. Let us define $\mu := \frac{\pi_\beta(x_0)}{\pi_\alpha(x_0)}$ as the ratio of the splitting probabilities of transition to β and α from the unstable equilibrium point ω. The ratio μ is a measure of the effectiveness of the transfer mechanism from α to β. From Monte Carlo simulations with $d = 150\ nm$, $x_0 = \omega$ and a duty ratio of 0.5, it is observed as expected that $\mu \sim 1$. To enable greater chances of the bead transitioning from α to β, a higher value of μ is desired. This can be achieved by increasing the duty ratio T_{ON}/T_{total} of laser at β (or decreasing the duty ratio of the laser at α). Monte Carlo simulations with $d = 150\ nm$ and $x_0 = \omega$ are used to obtain the variation of μ with duty ratios at $-d$ (i.e. the left well) which is demonstrated in Fig. 7. It is clearly evident that as duty ratio increases μ increases, indicating that the probability to transition into the β well increases (while probability to jump back into the α well decreases) rapidly as is seen in Fig. 7. Thus the ratio μ forms a metric to judge the effectiveness of a transport mechanism; the higher the μ, the better.

In the previous section it was demonstrated that a double well potential comprising of two identical wells is realized by multiplexing the laser at the two locations d and $-d$ with equal ON times. Unequal ON times of the laser enables the creation of two unequal potentials. This can be verified by averaging over time the instantanenous potential $V(x, r(t), l(t))$ to obtain an effective potential $\tilde{V}(x)$ with both wells having different energies. Thus, modulation of the ON times is equivalent to tilting of the effective potential

$\tilde{V}(x)$. This tilting is used to enhance thermal noise based transfer of a particle from the shallower well to the deeper well. The next theorem presents a justification for noise induced transfer from the high energy well to low energy well due to unequal ON times of the laser at d and $-d$.

Theorem 4.2: If α and β represent the stable equilibrium points in the potential $W(x)$ as shown in Fig. 6 such that $W(\alpha) > W(\beta)$ and both the wells are parabolic with widths σ_1 and σ_2 respectively, then the stationary probability distribution is given by $P_s(x) =$

$$\begin{cases} \frac{\exp[\frac{W(\beta)-W(\alpha)-(1/2)W''(\alpha)(x-\alpha)^2}{k_BT}]}{\sqrt{\frac{2\pi k_BT}{W''(\beta)}}\,\mathrm{erf}\,[\sigma_2\sqrt{\frac{W''(\beta)}{2k_BT}}]+\sqrt{\frac{2\pi K_BT}{W''(\alpha)}}\exp[W(\beta)-W(\alpha)]\,\mathrm{erf}\,[\sigma_1\sqrt{\frac{W''(\alpha)}{2k_BT}}]}, \\ \text{if } |x-\alpha|<\sigma_1, \\ \frac{\exp[\frac{W(\alpha)-W(\beta)-(1/2)W''(\beta)(x-\beta)^2}{k_BT}]}{\sqrt{\frac{2\pi k_BT}{W''(\alpha)}}\,\mathrm{erf}\,[\sigma_1\sqrt{\frac{W''(\alpha)}{2k_BT}}]+\sqrt{\frac{2\pi K_BT}{W''(\beta)}}\exp[W(\alpha)-W(\beta)]\,\mathrm{erf}\,[\sigma_2\sqrt{\frac{W''(\beta)}{2k_BT}}]}, \\ \text{if } |x-\beta|<\sigma_2. \end{cases} \tag{12}$$

Proof: Given $W(x) =$

$$\begin{cases} W(\alpha)+\frac{1}{2}W''(\alpha)(x-\alpha)^2, \text{ if } |x-\alpha|<\sigma_1 \\ W(\beta)+\frac{1}{2}W''(\beta)(x-\beta)^2, \text{ if } |x-\beta|<\sigma_2 \end{cases} \tag{13}$$

Using $P_s(x) = C\exp[\frac{-W(x)}{k_BT}]$,

$$P_s(x) = \begin{cases} C\exp[-\frac{W(\alpha)}{k_BT} - \frac{\frac{1}{2}W''(\alpha)(x-\alpha)^2}{k_BT}], \text{ if } |x-\alpha|<\sigma_1 \\ C\exp[-\frac{W(\beta)}{k_BT} - \frac{\frac{1}{2}W''(\beta)(x-\beta)^2}{k_BT}], \text{ if } |x-\beta|<\sigma_2 \end{cases}$$

Then, $\int_{-\infty}^{\infty} P_s(x)dx = 1$ leads to $C^{-1} = \sqrt{\frac{2\pi k_BT}{W''(\alpha)}}\exp[-\frac{W(\alpha)}{k_BT}] + \sqrt{\frac{2\pi k_BT}{W''(\beta)}}\exp[-\frac{W(\beta)}{k_BT}]$. Substituting C in the expression for $P_s(x)$ leads to the result. ■

When $W(\alpha) - W(\beta) >> 0$, then

$$P_s(x) \sim \begin{cases} 0, \text{ otherwise} \\ \frac{\exp[\frac{-W''(\beta)(x-\beta)^2}{2k_BT}]}{\sqrt{\frac{2\pi K_BT}{W''(\beta)}}\,\mathrm{erf}\,[\sigma_2\sqrt{\frac{W''(\beta)}{2k_BT}}]}, \text{ if } |x-\beta|<\sigma_2 \end{cases} \tag{14}$$

The above analysis holds even in the of presence of an intermediate no force zone, as the potential energy of the entire zone is higher as compared to the wells and hence the probability of being in that zone is negligible. In steady state the particle will be in the β well if the energy gap between the two wells is extremely large. It is interesting to note that although the potential $W(x)$ in Fig. 6 has two stable equilibrium points; in steady state all trajectories end up in the well with the lowest energy with significantly high probability. Thus even though we have multiple stable equilibrium points (with different energies), effectively in steady state only one "equilibrium" point is effective when noise is present. We emphasize that the noise, therefore, makes it possible to induce transport in a desired direction which would be absent in a deterministic system. Also note that the depth of all the wells is sufficient to trap cargo (the transport would not be remarkable if one of the wells is marginally stable; in which case it is intuitive to expect the transport to the deeper well).

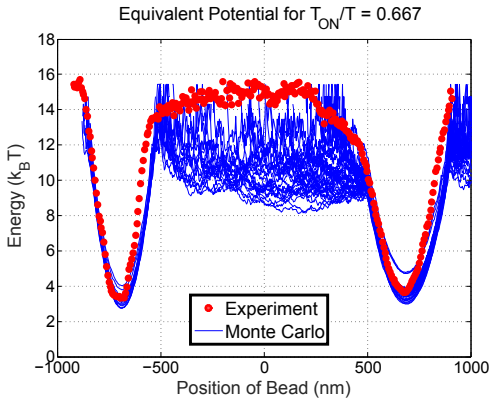

Fig. 8. Equivalent Potential for $\frac{T_{ON}}{T_{total}} = 0.667$ obtained using Monte Carlo simulation and Experiments. Close match between experimental and Monte Carlo simulations is seen.

Validation of the theoretical analysis is presented below using Monte Carlo simulations and experiments. Equations (7), (8) and (9) with unequal ON times are used as model for a bead in an effective double well potential.

It is desired that the bead, initially in the well at d transfers to the well at $-d$. Hence, $r(t) = 1$ for a shorter duration as compared to $l(t)$ in a single cycle of focusing of the laser at d and $-d$. The laser is focused at d for 80 μs and at $-d$ for 160 μs; where the net cycle lasts for 240 μs (duty ratio $T_{ON}/T = 0.667$). Simulation results with 100 particles for a duration of 200 seconds are shown in Fig. 8. It is seen that the effective potential on the left is slightly deeper as compared to one on the right. To see if higher duty ratio corresponds to more tilting, simulation results for transferring the bead from the right to left well for duty ratio $= 0.833$ are shown in Fig. 9. The duration is 20 seconds as compared to 200 seconds for the 0.667 duty ratio case. It is observed that for more than 90% of the particles to transfer to the left well, it takes 20 seconds for duty ratio of 0.833 as compared to 200 seconds for the duty ratio $= 0.667$ case. Thus, a higher duty ratio enables a faster transfer of particles owing to higher μ. Experimental results corresponding to these cases are shown in Fig. 8 and Fig. 9. It is seen that the effective potentials reconstructed from Monte Carlo simulations and experiments match closely. The tilting of the effective potential $\tilde{V}(x)$ is seen clearly, with the difference between the depths of two wells greater in Fig. 9 than in Fig. 8. This method of nanoscale transport has also been applied to transport a bead across three wells as well as to transport multiple beads but are not presented here due to space constraints.

V. CONCLUSIONS

Model for a single well potential was developed with experimentally derived parameters and subsequently used to quantitatively predict the optical forces felt by the bead under a wide variety of optical field manipulation and different energy profiles, such as a double well potential. It was shown that the dynamics of a bead in a double well potential $V(x, r(t), l(t))$, realized by multiplexing a single laser at a high frequency, can be analyzed by using the effective potential $\tilde{V}(x)$ obtained by averaging over the instantaneous potential profiles. A strong match of Monte Carlo simulations

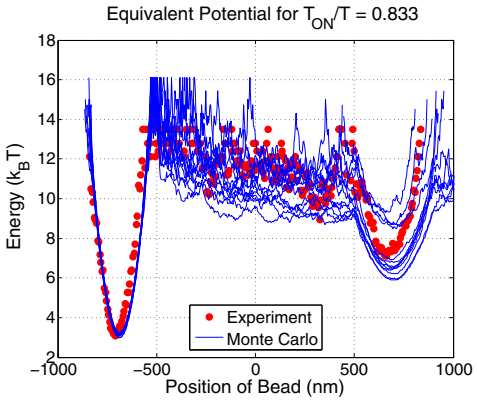

Fig. 9. Equivalent Potential for $\frac{T_{ON}}{T_{total}} = 0.833$ obtained using Monte Carlo simulations and experiments. Model predictions match experimental observations.

and experimental results was observed. The modeling opens up possibilities for using systems persoectives that are very effective in other nanotechnology platforms ([28], [29]). The models quantitatively capture how noise can play a role in transport of particles over micrometer spatial scales, enabling a methodology to obtain directed transport between two locations by multiplexing the laser for unequal times at each location. This demonstrated a means to achieve transport of a bead induced by thermal noise, providing a simple strategy based on modulating duty ratios of the laser multiplexing. Analytical justification for directed transport based on Kramer's time and splitting probabilities was presented. The explicit strategy was then experimentally implemented and a remarkable agreement with Monte Carlo simulations was found. It is observed that higher the duty ratio of the laser multiplexing at the location to be transferred, faster the transfer. Applications of this methodology to transfer across multiple locations as well as transport of multiple particles were experimentally demonstrated.

VI. Acknowledgements

The research reported in the article was partially supported by Natiional Science Foundation under the grants, CNS 1544721 and CMMI- 1462862. The authors acknowledge the support of University of Minnesota Supercomputing Institute (MSI) for lending their resources.

References

[1] K. Sekimoto, *Stochastic Energetics*. Springer, 2010, vol. 799.
[2] A. Caspi, R. Granek, and M. Elbaum, "Enhanced diffusion in active intracellular transport," *Physical Review Letters*, vol. 85, no. 26, p. 5655, 2000.
[3] O. M. Wilson, X. Hu, D. G. Cahill, and P. V. Braun, "Colloidal metal particles as probes of nanoscale thermal transport in fluids," *Physical Review B*, vol. 66, no. 22, p. 224301, 2002.
[4] S. Roychowdhury, G. Saraswat, S. Salapaka, and M. Salapaka, "On control of transport in brownian ratchet mechanisms," *Journal of Process Control*, vol. 27, pp. 76–86, 2015.
[5] J. Parrondo and B. J. de Cisneros, "Energetics of brownian motors: a review," *Applied Physics A*, vol. 75, no. 2, pp. 179–191, 2002.
[6] S. Ramaswamy, R. Lakerveld, P. I. Barton, and G. Stephanopoulos, "Controlled formation of nanostructures with desired geometries: Part 3. dynamic modeling and simulation of directed self-assembly of nanoparticles through adaptive finite state projection," *Industrial & Engineering Chemistry Research*, vol. 54, no. 16, pp. 4371–4384, 2015.
[7] A. Ashkin, J. Dziedzic, J. Bjorkholm, and S. Chu, "Observation of a single-beam gradient force optical trap for dielectric particles," *Optics letters*, vol. 11, no. 5, pp. 288–290, 1986.
[8] D. G. Grier, "A revolution in optical manipulation," *Nature*, vol. 424, no. 6950, pp. 810–816, 2003.
[9] C. S. Peskin, G. M. Odell, and G. F. Oster, "Cellular motions and thermal fluctuations: the brownian ratchet." *Biophysical journal*, vol. 65, no. 1, p. 316, 1993.
[10] P. T. Korda, M. B. Taylor, and D. G. Grier, "Kinetically locked-in colloidal transport in an array of optical tweezers," *Physical review letters*, vol. 89, no. 12, p. 128301, 2002.
[11] J. Krumhansl and J. Schrieffer, "Dynamics and statistical mechanics of a one-dimensional model hamiltonian for structural phase transitions," *Physical Review B*, vol. 11, no. 9, p. 3535, 1975.
[12] Y. T. Chang and W. H. Miller, "An empirical valence bond model for constructing global potential energy surfaces for chemical reactions of polyatomic molecular systems," *Journal of Physical Chemistry*, vol. 94, no. 15, pp. 5884–5888, 1990.
[13] U. Weiss, *Quantum Dissipative Systems*. World Scientific, 1999, vol. 10.
[14] R. Landauer, "Irreversibility and heat generation in the computing process," *IBM journal of research and development*, vol. 5, no. 3, pp. 183–191, 1961.
[15] A. Bérut, A. Arakelyan, A. Petrosyan, S. Ciliberto, R. Dillenschneider, and E. Lutz, "Experimental verification of landauer/'s principle linking information and thermodynamics," *Nature*, vol. 483, no. 7388, pp. 187–189, 2012.
[16] C. Jarzynski, "Nonequilibrium equality for free energy differences," *Physical Review Letters*, vol. 78, no. 14, p. 2690, 1997.
[17] A. Ranaweera and B. Bamieh, "Modelling, identification, and control of a spherical particle trapped in an optical tweezer," *International Journal of Robust and Nonlinear Control*, vol. 15, no. 16, pp. 747–768, 2005.
[18] C. W. Gardiner *et al.*, *Handbook of Stochastic Methods*. Springer Berlin, 1985, vol. 4.
[19] S. Roychowdhury, S. Bhaban, S. Salapaka, and M. Salapaka, "Design of a constant force clamp and estimation of molecular motor motion using modern control approach," in *American Control Conference (ACC), 2013*. IEEE, 2013, pp. 1525–1530.
[20] S. Roychowdhury, T. Aggarwal, S. Salapaka, and M. V. Salapaka, "High bandwidth optical force clamp for investigation of molecular motor motion," *Applied Physics Letters*, vol. 103, no. 15, p. 153703, 2013.
[21] K. Sekimoto, "Langevin equation and thermodynamics," *Progress of Theoretical Physics Supplement*, vol. 130, pp. 17–27, 1998.
[22] D. S. Lemons and P. Langevin, *An introduction to stochastic processes in physics*. JHU Press, 2002.
[23] F. Reif, *Fundamentals of statistical and thermal physics*. Waveland Press, 2009.
[24] M. Huber, R. Perkins, A. Laesecke, D. Friend, J. Sengers, M. Assael, I. Metaxa, E. Vogel, R. Mareš, and K. Miyagawa, "New international formulation for the viscosity of h_2o," *Journal of Physical and Chemical Reference Data*, vol. 38, no. 2, pp. 101–125, 2009.
[25] L. I. McCann, M. Dykman, and B. Golding, "Thermally activated transitions in a bistable three-dimensional optical trap," *Nature*, vol. 402, no. 6763, pp. 785–787, 1999.
[26] T. Aggarwal and M. Salapaka, "Real-time nonlinear correction of back-focal-plane detection in optical tweezers," *Review of Scientific Instruments*, vol. 81, no. 12, p. 123105, 2010.
[27] K. Sekimoto, "Kinetic characterization of heat bath and the energetics of thermal ratchet models," *Journal of the physical society of Japan*, vol. 66, no. 5, pp. 1234–1237, 1997.
[28] D. R. Sahoo, T. De Murti, and M. V. Salapaka, "Observer based imaging methods for atomic force microscopy," in *Decision and Control, 2005 and 2005 European Control Conference. CDC-ECC'05. 44th IEEE Conference on*. IEEE, 2005, pp. 1185–1190.
[29] A. Sebastian, D. R. Sahoo, and M. V. Salapaka, "An observer based sample detection scheme for atomic force microscopy," in *Decision and Control, 2003. Proceedings. 42nd IEEE Conference on*, vol. 3. IEEE, 2003, pp. 2132–2137.